Modification of ATRP Surface-Initiated Poly(hydroxyethyl methacrylate) Films with Hydrocarbon Side Chains

Eric L. Brantley, Tracy C. Holmes, and G. Kane Jennings*

Department of Chemical Engineering, Vanderbilt University, Nashville, Tennessee 37235

Received: June 3, 2004; In Final Form: July 26, 2004

Poly(2-hydroxyethyl methacrylate) (PHEMA) films were grown onto gold via water-accelerated, surface-initiated atom transfer radical polymerization (ATRP), and the resulting side chains were modified by reaction with alkanoyl chlorides ($C_mH_{2m+1}COCl$; $m = 1$, 7, 11, 13, 15, and 17) to incorporate hydrocarbon side groups within the film. We have previously demonstrated the ability to react ∼70−80% of PHEMA hydroxyl side chains with fluorocarbon acid chlorides to prepare partially fluorinated films. Here we convert the side chains to hydrocarbon esters with diminishing conversion (80 to 40%) as *m* is increased and compare the resulting films with fluorocarbon-modified PHEMA. Based on IR spectra and wetting data, hydrocarbon side chains structure the film to a greater extent as *m* is increased. A critical chain length ($m = 15$) was required to orient chains normal to the interface at the outer film surface and impart the wetting properties of a dense methyl surface. The resistances of the films against the transport of redox probes were greatly enhanced with increasing conversion of hydroxyl groups within the film and were modestly affected by film structuring to create a densely packed methyl surface. For example, capping the hydroxyl groups of PHEMA by reaction with acetyl chloride resulted in an unstructured film with >90% conversion that increased film resistance by almost four orders of magnitude over the base PHEMA film without a significant volumetric enhancement of the side chains. Also, the decreasing conversion as *m* is increased from 7 to 17 resulted in a decreasing film resistance even though the longer chains structured the film and surface to a greater extent. These results illustrate the important effect on barrier properties of unreacted hydroxyl groups, which possibly associate to create water and ion-diffusing pathways within the film. The barrier properties of these hydrocarbon-modified PHEMA films are comparable to those of fluorocarbon-modified PHEMA when both conversion and the molecular weight of the modifying group are similar.

Introduction

In comparison with traditional processes used to prepare polymer coatings, surface-initiated polymerization methods provide numerous advantages, including chemical attachment of the polymer to the surface,[1] preparation of conformal coatings on objects of various shape,[2] good control over film thickness and composition,[3] and ease of patterning.[4,5] Much of the initial work in this area has focused on thin-film synthesis to impact materials applications, such as membrane[6] or chromatographic[7] separations, nanostructure modification,[8,9] and etch-resistant, patterned films.[4,5] In these applications, the surface and barrier properties of the polymer films are of utmost importance, and the ability to control surface and bulk film composition through molecular engineering of functional groups can have a significant impact on film performance.[6,10]

This manuscript examines the role of hydrocarbon side-chain length and conversion on the structural, surface, and barrier properties of surface-initiated polymer films. Hydrocarbon polymers are potentially useful in thin-films applications because they are inert, available at low cost, and resistant to penetration by moisture.[11−15] However, many hydrocarbon polymers, such as polyethylene, are extremely difficult to process into ultrathin films due to solubility issues.[16] A goal of our work here is to prepare polymer films that exhibit hydrocarbon-like surface and barrier properties but are actually prepared via straightforward surface-initiated strategies. Since surface and barrier properties are ultimately important in many applications, a fundamental understanding of how hydrocarbon side-chain length affects these properties would be advantageous in the molecular-level design of polymer films.

We prepare these films using a two-step procedure that consists first of water-accelerated, surface-initiated atom transfer radical polymerization (ATRP)[3,9,17−21] followed by reaction of the grown film with a hydrocarbon species to introduce functionality. The advantages of this approach are that the polymer film is covalently attached to an initiator molecule on the surface, a tremendous amount of control of film growth kinetics over a wide thickness range is achieved by performing ATRP in water,[3,19] and film composition can be tailored by simple reaction to add appropriate molecular groups.[3,6,10,21] This methodology allows us to use a base film as a test stage for creation of numerous polymer films with varying chemical composition.

The surface-initiated growth of polymer films via ATRP typically exhibits sluggish kinetics that limit film thickness,[1,22,23] but the solution polymerization of a hydrophilic, water-soluble monomer may be accelerated by using water as solvent.[17,18] For the surface-initiated case, rather thick films (>100 nm) can now be grown in a controlled fashion using water-accelerated ATRP.[3,19] However, since acrylates or methacrylates having long alkyl side chains are not hydrophilic, the surface-initiated ATRP

* To whom correspondence should be addressed: e-mail: jenningk@vuse.vanderbilt.edu.

10.1021/jp0476038 CCC: $27.50
Published on Web 09/16/2004

SCHEME 1: Acylation of PHEMA with Hydrocarbon Acid Chlorides

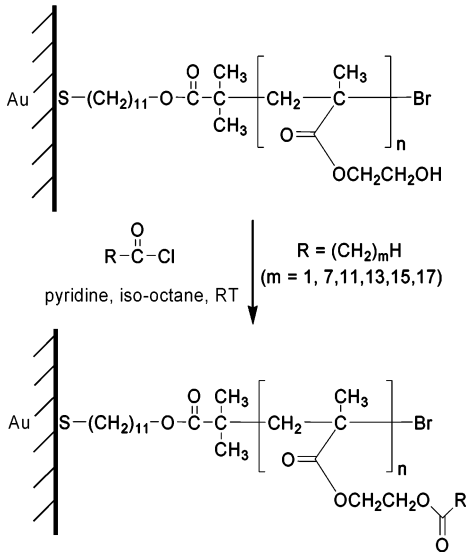

of such monomers would not likely produce films that are sufficiently thick to be effective barriers.[24] To achieve much thicker hydrocarbon films, we first polymerize the water-soluble, hydrophilic monomer hydroxyethyl methacrylate (HEMA) via water-accelerated, surface-initiated ATRP.[3,10,19] This method results in the controlled growth of moderately thick (>100 nm) PHEMA films. To gain even more control over film characteristics and to produce hydrocarbon-rich films, the hydroxyl-terminated side chains throughout the PHEMA film are reacted to introduce desirable chemical functionality. Huang et al.[3] previously reacted PHEMA with short hydrocarbon acid chlorides, thus demonstrating the ability to introduce groups into the polymer film via a simple acylation reaction of the side chains. Other recent work has exploited the hydroxyl groups of PHEMA by reaction with trimethylchlorosilane to make the film more hydrophobic and improve its etching resistance.[5] Additionally, modification of hydroxyl groups with $C_{15}H_{31}COCl$ has been shown to dramatically improve surface hydrophobicity of thin ($\leq$40 nm) surface-initiated polyglycidol brushes grown via anionic ring-opening polymerization on silicon.[25]

We have previously investigated the reaction of hydroxyl groups of PHEMA with fluorocarbon acid chlorides and extensively analyzed the structure and composition of the films as well as the surface and barrier properties.[10] We observed that a longer fluorocarbon side chain (of length 7) imparted structure to the film, both at the surface where the chains align along the normal at the air−film interface and also in the bulk where the chains pack to maximize interchain interactions, whereas a shorter fluorocarbon chain (of length 3) offered little or no structuring. The current work conducts the same modification but uses hydrocarbon acid chlorides ($CH_3(CH_2)_{m-1}COCl$; m = 1, 7, 11, 13, 15, and 17; Scheme 1), allowing the comparison of film properties as a function of side-group composition, chain length, and molecular weight. Analogous to the work with fluorocarbon side chains, we identify hydrocarbon chain lengths that give structure to the polymer films at the surface and in the bulk.

Other work has been done on films containing long hydrocarbon chains. Kraft and Moore[26] have investigated the effects of reacting PHEMA microgels with hydrocarbon acid chlorides (m ranging from 1 to 15) to form fatty acid layers that delay microgel expansion. They found that acetyl-modified and unmodified microgels expand readily, that rather short (m = 4) alkyl chains offer maximum resistance to microgel expansion, and that as the chain length is further increased the resistance decreases. Varying alkyl side chain length has also been tested on Langmuir−Blodgett films, specifically investigating the role of chain length on the structure and order of the film packing. Of particular relevance, acylethylenimines having short hydrocarbon side chains were found to exist in an easily compressible, liquid-like state.[27] As the side-chain length was increased, the monolayers became more condensed, until at chain lengths greater than 13, the resulting monolayers became crystallized, rigid structures. Similarly, a hydrocarbon side chain length of 18 in polyimide Langmuir−Blodgett films resulted in crystallized structures, as verified by IR peak positions for methylene stretching modes.[28] As for surface-initiated polymers, Stöhr and Rühe[29] grew various *n*-alkyl methacrylates from physisorbed poly(caprolactone) macroinitiators on silicon oxide. They found that the surface became increasingly hydrophobic as the length of the polymer side chain was increased from a methyl to a stearyl group. However, to our knowledge, the combined structural, surface, and barrier properties of polymer films with varying alkyl side chain length have not been investigated. Our general film preparation methods allow us to make these film property comparisons among various hydrocarbon-modified films produced in this work along with comparisons to our previously reported fluorocarbon-modified PHEMA films.

Experimental Section

Materials. CuCl (99.995+%), $CuBr_2$ (99.999%), 2,2′-bipyridine (bpy, 99+%), 2-hydroxyethyl methacrylate (HEMA, >99%), pyridine (99+%), lauroyl chloride ($C_{11}H_{23}COCl$, 98%), myristoyl chloride ($C_{13}H_{27}COCl$, 97%), palmitoyl chloride ($C_{15}H_{31}COCl$, 98%), $K_3Fe(CN)_6$ (99+%), $K_4Fe(CN)_6{\cdot}3H_2O$ (99%), and hexadecane (99%) were used as received from Aldrich. *N*,*N*-Dimethylformamide (DMF, 99.9%), isooctane (99%), acetyl chloride (CH_3COCl, 98%), octanoyl chloride ($C_7H_{15}COCl$, 99%), stearoyl chloride ($C_{17}H_{35}COCl$, >99%), and Na_2SO_4 (anhydrous) were used as received from Fisher. Gold shot (99.99%) and chromium-coated tungsten filaments were obtained from J&J Materials and R. D. Mathis, respectively. Silicon (100) wafers (Montco Silicon) were rinsed with ethanol and deionized water and dried with nitrogen. Ethanol (AAPER, absolute) was used as received. Deionized water (16.7 MΩ·cm) was purified with a Modu-Pure system and used as a solvent during polymerization and for rinsing. An initiator-terminated disulfide, $(BrC(CH_3)_2COO(CH_2)_{11}S)_2$, was synthesized as described in the literature.[4]

Preparation of Gold Substrates. Gold substrates were prepared by evaporating chromium (100 Å) and gold (1250 Å) in sequence onto silicon (100) wafers at rates of 1−2 Å s^{-1} in a diffusion-pumped chamber with a base pressure of 4×10^{-6} Torr. After removal from the evaporation chamber, the wafers were typically cut into 1 cm × 3 cm pieces.

Polymerization. Gold substrates were first placed in a 1 mM ethanol solution of $(BrC(CH_3)_2COO(CH_2)_{11}S)_2$ for 24 h. The initiated samples were then rinsed with ethanol, dried with nitrogen, and placed in vials that were subsequently degassed and backfilled with nitrogen. A Cu^{I}/Cu^{II}/bpy (69 mM CuCl, 20 mM $CuBr_2$, 195 mM bpy) system in a 50:50 v:v water/HEMA solution was used for polymerization.[3] The mixture was placed in a Schlenk flask sealed with a rubber septum and was degassed by performing three freeze−pump−thaw cycles. This was followed by transfer of the solution via cannula into vials containing up to six samples each. After polymerizing for 12 h at room temperature, the samples were thoroughly rinsed with

water and DMF and then dried with nitrogen. As measured by ellipsometry with samples from three different batches, PHEMA film thicknesses were 217 ± 11 nm under these conditions.

Film Acylation. Gold surfaces with PHEMA films were exposed to 20 mM solutions of acetyl chloride (CH_3COCl), octanoyl chloride ($C_7H_{15}COCl$), lauroyl chloride ($C_{11}H_{23}COCl$), myristoyl chloride ($C_{13}H_{27}COCl$), palmitoyl chloride ($C_{15}H_{31}COCl$), or stearoyl chloride ($C_{17}H_{35}COCl$) with 25 mM pyridine in isooctane for 24 h to give PHEMA films with acylated side chains (Scheme 1). The concentration of 20 mM is near or above the solubility limit of the longer-chain acid chlorides in isooctane. After reaction, the films were rinsed with isooctane and ethanol and dried with nitrogen. The various alkyl-modified PHEMA films are referred to by the length of the hydrocarbon chain (i.e. $C_7H_{15}COCl$-modified PHEMA is H7).

Characterization Methods. Polymer film properties were evaluated using the following methods before acylation to provide a baseline measurement and once again after acylation to track changes in film properties. Reflectance absorption infrared spectroscopy (RAIRS) was performed using a Bio-Rad Excalibur FTS-3000 infrared spectrometer. The p-polarized light was incident at 80° from the surface normal. The instrument was run in single reflection mode and equipped with a Universal sampling accessory. A liquid-nitrogen-cooled, narrow-band MCT detector was used to detect reflected light. Spectral resolution was 2 cm^{-1} after triangular apodization. Each spectrum was accumulated over 1000 scans using a deuterated octadecanethiol-d_{37} self-assembled monolayer on gold as the background.

Ellipsometry measurements were taken on a J. A. Woollam Co. M-2000DI variable angle spectroscopic ellipsometer with WVASE32 software for modeling. Measurements at three spots per sample were taken with light incident at a 75° angle from the surface normal using wavelengths from 400 to 800 nm. Optical constants for a bare gold substrate, cut from the same wafer as the samples to be characterized, were measured by ellipsometry and used as the baseline for all polymer film samples. Film thickness of the polymer layer on samples, regardless of modification, was obtained using a two-term Cauchy layer model, allowing the modeling software to fit thickness as well as the two Cauchy terms defining the refractive index, *n*. Typical values for *n* from the modeling software ranged between 1.45 and 1.50. Film thicknesses reported herein are generally lower but believed to be more accurate than in our previous work[10] due to changes in our ellipsometry procedures.

A Rame-Hart contact angle goniometer with a microliter syringe was used to measure advancing and receding contact angles on static drops of water and hexadecane on the polymer surfaces. The needle tip of the syringe remained inside the liquid drop while measurements were taken on both sides of ~5 μL drops. Reported values and ranges represent the average and standard deviation of values obtained from at least five independent sample preparations.

Electrochemical impedance spectroscopy (EIS) was performed with a Gamry Instruments CMS300 impedance system interfaced to a personal computer. A flat-cell (EG&G Instruments) was used to expose only 1 cm^2 of each sample to an aqueous solution containing electrolyte and redox probes while preventing sample edges from being exposed. The electrochemical cell consisted of an aqueous solution of 1 mM $K_3Fe(CN)_6$, 1 mM $K_4Fe(CN)_6 \cdot 3H_2O$, and 0.1 M Na_2SO_4 with a Ag/AgCl/saturated KCl reference electrode, a gold substrate counter electrode, and a gold substrate containing the film to be studied as the working electrode. All data were collected in the range from 10^{-1} to 10^4 Hz using 10 points per decade and were fit with an appropriate equivalent circuit model (vide infra) to determine resistance and capacitance values. Reported values and ranges for resistance and capacitance represent the average and standard deviation of values obtained from at least four independent sample preparations.

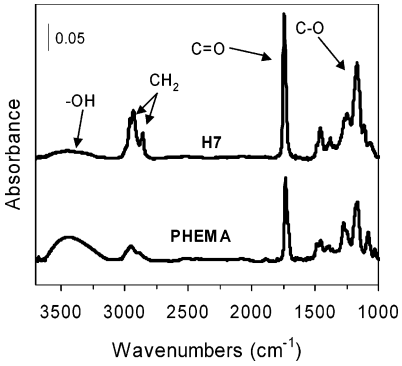

Figure 1. Reflectance absorption IR spectra of PHEMA and a representative hydrocarbon-modified PHEMA sample, H7. Regions of interest are labeled on the plot.

TABLE 1: Position (cm^{-1}) of Selected IR Peaks and Average Conversion for Modified PHEMA Films

film	ν (C=O)[a]	ν_s (CH_2)	ν_a (CH_2)	χ (%)
H1	1750			93 ± 3
H7	1744	2858	2930	82 ± 5
H11	1744	2855	2926	77 ± 6
H13	1742	2855	2925	68 ± 5
H15	1742	2852	2922	64 ± 4
H17	1737	2852	2921	37 ± 6
H17/H1	1750	2852	2920	82 ± 4

[a] These positions are typical for each film but can shift slightly as conversion deviates from the average values.

Results and Discussion

Film Composition and Structure. We used RAIRS to monitor compositional changes within the polymer films due to acylation by the various acid chlorides. Figure 1 shows a survey IR spectrum for a representative hydrocarbon-modified PHEMA film, H7, along with the spectrum for PHEMA. All other films exhibit the same peaks in the IR spectrum as H7 but at slightly different positions and intensities. The most readily quantifiable change in the spectra that is indicative of successful acylation is diminution of the hydroxyl peak in the region from 3100 to 3700 cm^{-1}, as the hydroxyl side chains of PHEMA are converted to esters. We have used the diminution of integrated hydroxyl peak area (A_{OH}) to estimate conversion (χ) of the hydroxyl side chains as

$$\chi = 1 - \frac{A_{\text{OH, acylated PHEMA}}}{A_{\text{OH, PHEMA}}} \quad (1)$$

which assumes that any change in integrated hydroxyl peak area is due solely to acylation and not to orientational changes of unreacted hydroxyl groups. Table 1 lists conversions, calculated using Eq 1, from at least five independent preparations for each acid chloride. As the chain length of the hydrocarbon side chain is increased, conversion drops substantially, suggesting that molecular size limits penetration and subsequent reaction of acid chlorides within the film. For the modification with the longest side group (H17), conversion was significantly lower than that for the other hydrocarbon films. Several attempts were made, without success, to increase conversion for H17 by using

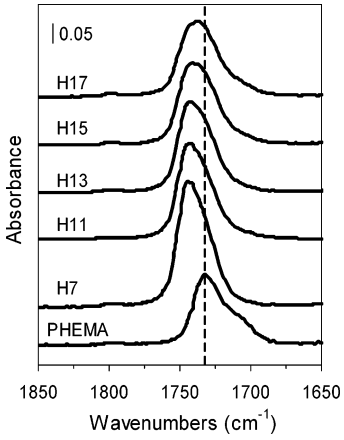

Figure 2. Carbonyl stretching region of IR spectra for PHEMA and hydrocarbon-modified PHEMA films. The dashed line is at 1733 cm^{-1}, the position of the carbonyl peak for PHEMA.

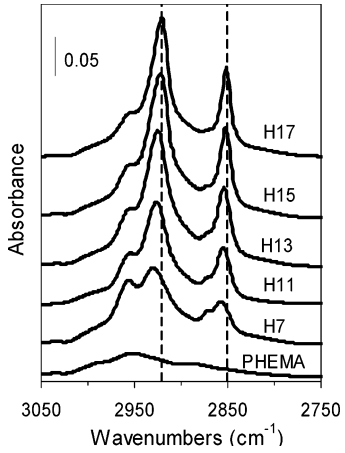

Figure 3. C−H stretching region of IR spectra for PHEMA and hydrocarbon-modified PHEMA films. The dashed lines are positioned at 2852 and 2921 cm^{-1}, corresponding to the lowest peak positions observed for $\nu_s(CH_2)$ and $\nu_a(CH_2)$ in these films.

different solvents and raising temperature. For completeness, results for H1 and a copolymer film, H17/H1, are included in tables along with the other films. These films are not discussed until later in this section.

The acylation reaction studied here causes two other differences in the IR spectra of modified PHEMA films as compared to PHEMA: introduction of an additional ester linkage and the presence of hydrocarbon chains of varying length on each modified side chain. The hydrocarbon ester from acylation of the side chain results in a second carbonyl peak in the spectrum around 1750 cm^{-1} and enhanced C−O stretching peaks from 1100 to 1300 cm^{-1}. The introduction of long hydrocarbon chains into the polymer film results in a significant increase in the intensity of C−H bending (1400 to 1500 cm^{-1}) and C−H stretching (2800 to 3000 cm^{-1}) modes in the IR spectrum.

The carbonyl peak resulting from acylation is not easily distinguished from the original PHEMA ester carbonyl peak (Figure 2) due to a similar chemical environment and therefore similar peak positions. The peak for the carbonyl associated with the PHEMA ester appears at 1733 cm^{-1}, whereas the carbonyl peak due to acylation appears at somewhat higher wavenumbers (∼1750 cm^{-1}, as evidenced by this peak position for H1) but still relatively close to the PHEMA carbonyl peak. Upon acylation, one broader peak appears in the region, representing the combined intensities of the PHEMA carbonyl and the carbonyl from the acylation reaction. From Figure 2 and Table 1, the resultant carbonyl peak position shifts with increasing hydrocarbon chain length (m). This shift is due to lower conversion within the film as m increases, meaning that less IR peak intensity is introduced at higher wavenumbers by the new carbonyl. Furthermore, the overall intensity of the combined carbonyl peak is also reduced as m is increased because of diminishing conversion.

Addition of alkyl groups to the PHEMA side chains also results in a significant increase in C−H bending and stretching bands in the IR spectrum, and the position of these peaks gives an indication of chain packing and crystallinity. As compared to the spectrum for PHEMA (Figure 1), those for modified PHEMA show a sharper CH_2 bending peak at ∼1470 cm^{-1}. However, there is no peak splitting as observed in crystalline polymethylene lattices with orthorhombic chain packing.[16] Symmetric and asymmetric methylene stretching modes, $\nu_s(CH_2)$ and $\nu_a(CH_2)$ respectively, become much more prominent and sharper after addition of alkyl side chains (Figure 3). From previous IR studies of polymethylene chains,[16,30] a $\nu_s(CH_2)$ mode positioned at ∼2850 cm^{-1} and a $\nu_a(CH_2)$ mode positioned at ∼2918 cm^{-1} are indicative of highly crystalline chain packing while shifts to higher wavenumbers indicate less dense, more liquid-like packing.[31] Figure 3 shows that increasing the hydrocarbon chain length results in more crystalline chain packing (fewer gauche conformers) within the film as the $\nu_a(CH_2)$ position decreases from 2930 ($m = 7$) to 2921 ($m = 17$) cm^{-1}. The improved crystallinity observed for longer alkyl side groups is consistent with greater van der Waals interactions among hydrocarbon chains, which increase proportionally with chain length and facilitate chain structuring within the film.[32] Additionally, in copolymer systems having one component that packs efficiently and one that packs poorly (i.e. ethylene−butene copolymers[33]), the efficient-packing chains tend to order while the poorer-packing chains do not. In our system, increasing hydrocarbon chain length results in more crystalline packing because the van der Waals interactions between the alkyl chains become increasingly important as compared with the interactions between other groups within the polymer film.

Film Thickness. Table 2 shows film thicknesses obtained by ellipsometry before and after acylation with hydrocarbon acid chlorides. Starting with a PHEMA film, the polymer layer expands upon acylation with hydrocarbon acid chlorides to accommodate the additional side-chain volume. The observed trends roughly agree (within ∼30%) with theoretical estimates based on conversion and molecular weight considerations, which have been used previously[3] to model the addition of short hydrocarbon groups to PHEMA. With the exception of H17, which exhibits exceptionally low conversion, the addition of long hydrocarbon groups ($m = 7$ to 15) resulted in slightly more than a doubling of polymer film thickness. Since the hydrocarbon chains exhibit lower conversions from H7 to H15, the film thickness change remains relatively constant for this series.

Surface Wetting Properties. Advancing and receding contact angles (θ_A and θ_R) of water were measured for all polymer films to provide a measure of surface hydrophobicity. Table 3 gives average contact angles for the modified films along with the values for PHEMA and the bromine-terminated initiator monolayer for comparison. Both the advancing contact angle and the contact angle hysteresis ($\theta_A - \theta_R$) of water on the initiator are indicative of a smooth, bromine-terminated monolayer.[34] Once PHEMA is grown from the initiator, the advancing contact angle is not significantly altered, but the hysteresis becomes quite high, suggesting a rough and/or chemically heterogeneous surface. Hydrocarbon-modified PHEMA films ($m = 7-17$) show much higher advancing water contact angles, ranging from 104° to

TABLE 2: Thickness Change of PHEMA Films upon Acylation with Hydrocarbon Acid Chlorides

	thickness (nm)				
film	before	after	observed increase	repeat unit MW (g mol^{-1})	theoretical increase (MW)
H1	216	295	37%	172	30%
H7	215	452	110%	256	81%
H11	224	508	127%	312	116%
H13	205	458	124%	341	121%
H15	231	489	111%	369	119%
H17	231	322	40%	397	75%
H17/H1	208	318	53%	-	87%[a]

[a] Based on 35% conversion for H17 and 47% for H1.

TABLE 3: Water and Hexadecane Advancing and Receding Contact Angles (°) for Films on Gold

	water		hexadecane	
film	θ_A	θ_R	θ_A	θ_R
initiator	80 ± 2	74 ± 2	<10	<10
PHEMA	75 ± 3	23 ± 2	<10	<10
H1	70 ± 2	52 ± 3	<10	<10
H7	104 ± 2	60 ± 4	<10	<10
H11	113 ± 1	59 ± 4	16 ± 3	<10
H13	117 ± 1	70 ± 4	21 ± 2	<10
H15	117 ± 2	65 ± 5	44 ± 1	26 ± 3
H17	115 ± 3	77 ± 7	47 ± 2	34 ± 4

117°. Within this series, H7 gives a lower contact angle than the other films, indicating that the shorter chain is unable to fully affect surface properties. This effect is likely due to insufficient chain length. All other alkyl-modified films (H11 to H17) provide fairly high water contact angles, consistent with those reported for methyl-terminated surfaces.[34] Within this group, the lowest contact angle hysteresis is observed for H17 with the highest observed for H11, suggesting that longer alkyl side chains result in smoother or more homogeneous surfaces.

Contact angles of hexadecane were also measured on all polymer films. Hexadecane is a sensitive probe of hydrocarbon surface composition, indicating whether a surface consists primarily of $-CH_2-$ or $-CH_3$ groups. Well-structured methyl surfaces exhibit advancing hexadecane contact angles of ~50°, whereas hexadecane completely wets methylene surfaces.[35] Table 3 shows that the advancing hexadecane contact angle increases with increasing hydrocarbon side chain length. For H7, hexadecane completely wets the surface, indicating that $-CH_3$ groups are not at the surface of this film and remaining consistent with the lower advancing water contact angle. As the side chain is lengthened from $m = 11$ to 17, the hexadecane contact angle increases and approaches that for a purely methyl surface. For H11 and H13, the hexadecane contact angle is low, indicating that these surfaces contain a large proportion of methylene or ester groups with some methyl functionality as well. For H15 and H17, however, the higher hexadecane contact angles suggest that the surface consists almost entirely of $-CH_3$ groups. Dense methyl surfaces are only possible with modified PHEMA films if the added hydrocarbon side chains orient nearly normal to the air−film interface at the outer few angstroms.[36] These results are consistent with those from RAIRS, which indicate films with improved crystallinity as the hydrocarbon chain length is increased. Furthermore, other researchers[27] have noted an improvement in the crystallinity of acylethylenimine Langmuir−Blodgett films containing alkyl side chains having more than 13 carbons. We observe similar results here, particularly on the basis of RAIRS and hexadecane wetting results, with both H15 and H17 exhibiting superior crystalline packing and surface structuring as compared to films modified with shorter hydrocarbon groups.

For PHEMA modified with hydrocarbon as well as fluorocarbon chains, a critical chain length must first be selected to induce well-structured surfaces. From our previous work,[10] we found that modification of PHEMA with a fluorocarbon of chain length 3 (F3) does not structure the film very well at the outer surface but that modification using a chain length of 7 (F7) results in a densely packed, oriented fluorocarbon layer at the surface, exhibiting an extremely low critical surface energy (9 mN/m). For the hydrocarbon films here, alkyl chain lengths below 15 do not structure the surface to any great extent. However, modification with chain lengths of either 15 or 17 yield densely packed, oriented hydrocarbon surface layers analogous to dense fluorocarbon layers observed for F7. This offset in critical chain length was expected since, for Langmuir−Blodgett acylethylenimine films having either hydrocarbon or fluorocarbon side chains, longer hydrocarbon chains were required to achieve similar structure and air−film interfacial behavior as much shorter fluorocarbon chains.[27] The authors were unable to form LB films once a critical chain length was reached ($m >$ 13 for hydrocarbons and $m > 7$ for fluorocarbons), as these polymers tended to form crystallized structures that were difficult to transfer to a substrate. They attributed the shorter critical chain length to the increased rigidity and hydrophobicity for fluorocarbon chains. For modified PHEMA films, the much larger area occupied by fluorocarbon chains as compared to hydrocarbon chains (diameter of 5.6 Å compared to 4.2 Å, or 80% greater area)[37] and enhanced fluorocarbon rigidity likely result in a shorter critical chain length. In either case, these outermost groups orient normal to yield a mostly (perfluoro)methyl surface only when the chains are sufficiently long to achieve interchain van der Waals interactions and prevent chain collapse at the surface that would expose (perfluoro)methylene groups.

Barrier Properties. We investigated the barrier properties of modified PHEMA films having various hydrocarbon side chains using EIS upon exposure to 1 mM $K_3Fe(CN)_6$ and 1 mM $K_4Fe(CN)_6$ in 0.1 M Na_2SO_4(aq). Figure 4 shows EIS spectra in the form of Bode plots for the initiator, PHEMA, and all of the modified polymer films on gold. Solid curves in the plot represent best fits of the data with appropriate equivalent circuit models (Figure 5) to provide quantitative information (Table 4) on the effect of composition on film resistance and capacitance. The following terms are used to denote various film and solution characteristics: solution resistance, R_s; initiator capacitance, C_i; initiator resistance, R_i; total film (polymer plus

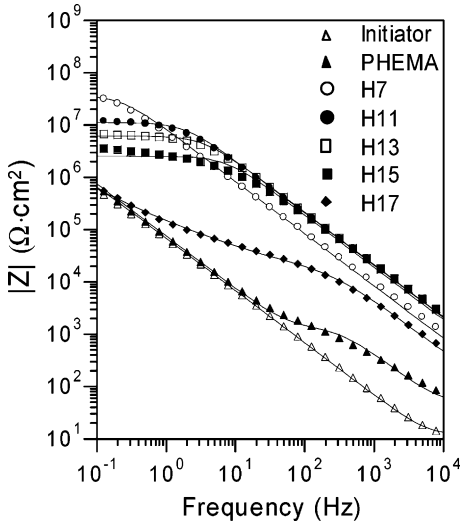

Figure 4. Electrochemical impedance spectra for films on gold obtained in 1 mM $K_3Fe(CN)_6$ and 1 mM $K_4Fe(CN)_6$ in 0.1 M Na_2SO_4(aq). Spectra are shown for PHEMA before and after modification with initiator-modified gold as a reference. Solid curves represent a fit of the data to an equivalent circuit.

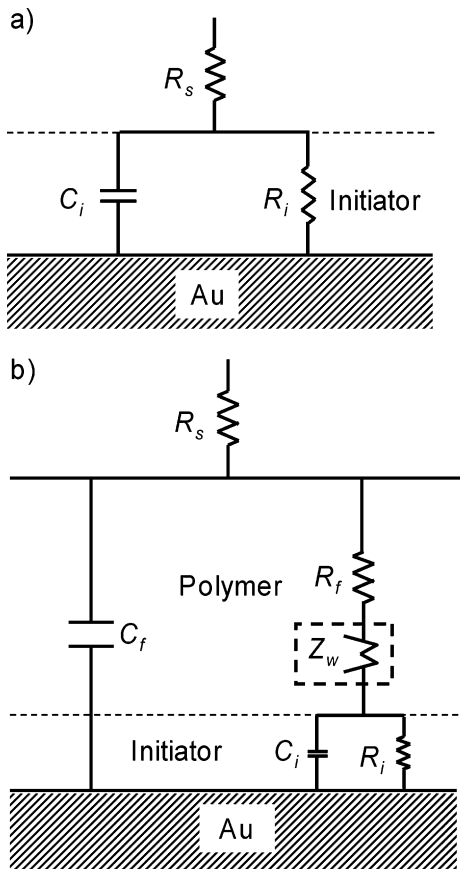

Figure 5. Equivalent circuit models used in analysis of impedance spectra for films on gold: (a) One-time-constant model for initiator, (b) Two-time-constant model for polymer films. For (b), when R_f dominates the combined impedance from R_i and C_i, the circuit simplifies to the simpler form of (a) but containing R_f and C_f. The dashed box contains a Warburg impedance that was only included in the model for H17.

initiator) capacitance, C_f, and polymer film resistance, R_f. Our previous work[10] includes extensive discussion of the impedance spectra for both bare gold and the initiator monolayer on gold.

As we have discussed previously,[10] the growth of a PHEMA film atop the initiator shows a second time constant (due to the polymer film) at high frequencies and is appropriately fitted with a more complex model (Figure 5b) obtained by adding R_f and C_f to the initiator equivalent circuit in Figure 5a. While this same equivalent circuit rigorously applies to the acylated PHEMA films studied here, only one time constant typically appears in their impedance spectra. For the hydrocarbon films other than H17, R_f is greater than the combined impedance of R_i and C_i in parallel, so only a single time constant due to the hydrocarbon-modified film is observed in the spectra. For these films, the equivalent circuit in Figure 5b simplifies to a Randles model having R_s in series with a parallel combination of R_f and C_f (similar to Figure 5a but replacing R_i with R_f and C_i with C_f). The impedance behavior of H17 (Figure 4), due to a poor fit with the basic two-time-constant model, requires use of a modified two-time-constant model created by adding a Warburg impedance (Z_w) term between R_f and the initiator circuit (indicated by the dashed box in Figure 5b).[38] The Warburg impedance term (Z_w) is used to represent a resistance to mass transfer[39] associated with the polymer film layer. The frequencies at which Z_w is observed lie between those where the initiator (low frequency, long time) and polymer (high frequency, short time) layers dominate. During these intermediate time scales, the diffusion of redox species through the polymer limits electron transfer.

TABLE 4: Capacitance and Resistance Values for PHEMA and Modified PHEMA Films

film	C_f (nF/cm^2)	log R_f (Ω ·cm^2)
PHEMA[a]	640 ± 200	3.0 ± 0.3
H1	20 ± 3	6.7 ± 0.8
H7	13.3 ± 4.8	7.0 ± 0.7
H11	9.2 ± 2.3	6.9 ± 0.3
H13	8.6 ± 2.1	6.7 ± 0.3
H15	9.1 ± 2.4	6.5 ± 0.3
H17[b]	25 ± 19	4.2 ± 0.4
H17/H1	11 ± 2	7.7 ± 0.2
F3[c]	12 ± 7	6.7 ± 0.5
F7[d]	9.2 ± 1.7	7.4 ± 0.4

[a,c,d] Values for PHEMA, C3F7−PHEMA, and C7F15−PHEMA, respectively.[10] [b] Log Z_w (Ω ·cm^2) for H17 was determined to be 5.0 ± 0.5.

Since impedance is directly proportional to film resistance and inversely proportional to film capacitance,[40] good barrier films are those having high R_f and low C_f. Table 4 contains R_f and C_f values obtained for all films studied. The impedance spectrum for PHEMA (Figure 4) merely shows a slight increase in impedance over that of the initiator monolayer at high frequencies, indicating the time constant for the polymer. The low film resistance ($\sim 10^3$) for PHEMA indicates rapid water and ion transport into the moderately hydrophilic film. As the PHEMA film is modified with hydrocarbon side chains, the impedance spectrum is observed to shift upward, due to a dramatically lower film capacitance (factor of 25 or greater) and a remarkable increase in film resistance (factor of $\sim 10^4$ except for H17) over PHEMA. Fits of the impedance data indicate minor drops in R_f as the hydrocarbon chain length is increased from 7 to 15 and a significant drop from 15 to 17 (Table 4). That the effect of chain length on film resistance is the opposite of that observed on film crystallinity and oleophobicity/hydrophobicity suggests that other film properties are influencing water and ion uptake. In terms of capacitance, C_f is 13 nF/cm^2 for H7, while C_f is about 9 nF/cm^2 for H11 through H15. These values are 50 to 70 times lower than C_f for PHEMA. This comparison is consistent with the increased film thicknesses after acylation and the lower film dielectric constant imparted by hydrocarbon chains.

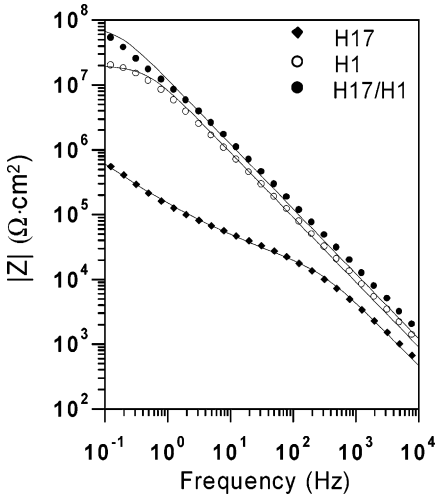

Figure 6. Electrochemical impedance spectra obtained in 1 mM $K_3Fe(CN)_6$ and 1 mM $K_4Fe(CN)_6$ in 0.1 M Na_2SO_4(aq) for H17, H1, and H17/H1 films on gold. Solid curves represent a fit of the data to an equivalent circuit.

The barrier properties of hydrocarbon-modified PHEMA films appear to be more closely related to side-chain conversion than to surface properties or crystallinity of the film. For instance, H7, though it is not a well-structured film and does not exhibit impressive wettability, has a higher conversion than the other hydrocarbon films and a slightly higher R_f. As the hydrocarbon chain length is increased, conversion becomes lower and R_f falls accordingly. Furthermore, H17, which yields the most structured air−film interface, exhibits a significantly reduced R_f as compared to the other hydrocarbons studied. These results suggest that merely eliminating hydroxyl groups from the film is a key to developing improved barriers from hydrocarbon-modified PHEMA films and that film structuring and surface wettability are of secondary importance. This finding is in contrast to our results for fluorocarbon-modified PHEMA films[41] where tremendous improvements in barrier properties were observed at low conversions ($\chi \sim 20\%$) and were correlated with the surface properties of the films. We attribute this phenomenon to differences in film structuring and hydrophobicity for fluorocarbon versus hydrocarbon chains.

To further examine the effect of conversion on impedance in hydrocarbon-modified films, we have used acetyl chloride to achieve high conversion for PHEMA and to cap unreacted hydroxyl groups in H17. Both PHEMA and H17 (with $\chi \sim 35\%$) films were placed in a 20 mM solution of acetyl chloride in isooctane to increase the conversion of hydroxyl groups to methyl esters (Table 1). The advancing and receding contact angles for water on H1 were consistent with a smoothing of the film as compared with PHEMA and a moderately hydrophilic surface (Table 3). When conversion for H17 was increased by backfilling with acetyl chloride to form H17/H1, no change was observed in surface properties, consistent with the dominance of oriented heptadecyl chains at the surface and a lower H1-rich region. Thickness changes for both H1 and H17/H1 (Table 2) exhibited only minimal increases (30−50%).

Figure 6 shows the impedance spectra for H1, H17, and H17/H1 while Table 4 summarizes the R_f and C_f values determined from fits of the data. Of particular importance, H1 exhibits a film resistance that is two orders of magnitude greater than that of H17 and almost four orders of magnitude greater than that of unmodified PHEMA. Since H1 contains no long alkyl side chains and exhibits minimal structuring, the improved impedance is due to high conversion in the capping of hydrophilic hydroxyl groups. The bulk film must have suppressed interactions with water, accomplished in our case by removal of hydrogen bonding moieties, to improve its resistance against the penetration by aqueous solutions. When unreacted, these hydroxyl groups may associate through hydrogen bonding to create water- and ion-diffusing pathways through the film. The elimination of these groups has a remarkable effect on resistance and capacitance while minimally affecting film thickness. Our work agrees with that of Zhou et al.,[5] who found that increasing the hydrophobic nature of PHEMA by reacting hydroxyl groups with trimethylchlorosilane greatly improved the resistance of the film to aqueous etching solutions.

We can use this capping approach to prepare films with optimal surface and barrier properties. For example, reacting H17 with acetyl chloride to produce H17/H1 yields a significantly reduced capacitance and the highest resistance of any film examined in this work (Table 4). In comparison with H7 (Table 4), which also has a χ of ~0.8, the H17/H1 film shows a factor of 5 higher resistance, which we attribute to the superior surface properties of H17/H1 over H7 that reduce water and ion penetration into the film. While comparison of H1 and H17 in Figure 6 yields the importance of conversion in elevating barrier performance, comparison of these two films with H17/H1 reveals that both high conversion within the film and the preparation of a well-structured, hydrophobic surface is required to optimize the barrier properties of a film.

In comparison with partially fluorinated PHEMA films generated in the same manner and exhibiting similar conversions,[10] the hydrocarbon films prepared here exhibit comparable barrier properties (see Table 4). The typical film resistance achieved with the hydrocarbon films is roughly 10^7 Ω·cm^2, with the best film (H17/H1) approaching 10^8 Ω·cm^2 and the best fluorinated films also approaching 10^8 Ω·cm^2.[10] The capacitances for both fluorocarbon and hydrocarbon films generally fall in the range of 10 nF/cm^2. Comparison between specific fluorinated films and hydrocarbon films can also be made based on side-chain length and molecular weight. Based on alkyl chain length, F7 provides higher R_f and lower C_f than H7, likely because of superior structuring at the surface and in the bulk even though H7 exhibits a bit higher χ (0.82 vs 0.67). In comparing side groups with similar molecular weight and conversion, H11 (MW = 312.4; χ = 0.77) and F3 (MW = 326.2; χ = 0.7) exhibit similar barrier properties. We also attempted to use benzoyl chloride to modify PHEMA, but unlike a fluoroaryl-modified PHEMA film that exhibits high conversion and excellent barrier properties,[10] the benzyl-modified film exhibited poor conversion and barrier properties.

Conclusions

The two-step polymerization/reaction method presented here represents a straightforward and effective way to create ultrathin films having various hydrocarbon side chains. The ability to grow PHEMA via a water-accelerated, surface-initiated scheme allows tremendous control over film thickness. Subsequent reaction of polymer side chains introduces hydrocarbon functionality into the film with diminishing conversion as the hydrocarbon chain length is increased. Increasing the hydrocarbon side-chain length increases the crystallinity of the hydrocarbon groups within the polymer films due to enhanced van der Waals interactions. Films having the longest chains, H15 and H17, yield wetting properties consistent with a densely packed methyl surface, indicating that the outermost groups are oriented nearly normal to the air−film interface. Shorter chains are unable to impart this degree of structure to the film. The

hydrocarbon films studied here could adequately be used in an application requiring an oleophobic/hydrophobic surface at much less cost than a fluorocarbon film. Tremendous improvement in film barrier properties was also observed upon acylation of PHEMA with hydrocarbon acid chlorides, but the improvement appears to be linked most closely to conversion of side chains while film structure and surface properties are secondary issues. The importance of conversion is illustrated by merely capping the hydroxyl groups of PHEMA with acetyl chloride to achieve $\chi \sim 90\%$ and four orders of magnitude improvement in film resistance. Nonetheless, the best barrier film prepared in this study, H17/H1, has both high conversion of hydroxyl groups (80%) and a densely packed hydrophobic methyl surface. Combined, the results described herein demonstrate the key roles of side chain composition and conversion in controlling film structure, surface properties, and barrier properties.

Acknowledgment. We gratefully acknowledge the National Science Foundation (CTS-0203183 and a NSF Graduate Research Fellowship (E.L.B.)) and the Vanderbilt University Summer Undergraduate Research Program (T.C.H.) for financial support. We also thank Dr. T. Randall Lee (University of Houston) for discussion surrounding fluorocarbon and hydrocarbon structuring.

References and Notes

(1) Matyjaszewski, K.; Miller, P. J.; Shukla, N.; Immaraporn, B.; Gelman, A.; Luokala, B. B.; Siclovan, T. M.; Kickelbick, G.; Vallant, T.; Hoffmann, H.; Pakula, T. *Macromolecules* **1999**, *32*, 8716−8724.

(2) Pyun, J.; Kowalewski, T.; Matyjaszewski, K. *Macromol. Rapid Commun.* **2003**, *24*, 1043−1059.

(3) Huang, W. X.; Kim, J. B.; Bruening, M. L.; Baker, G. L. *Macromolecules* **2002**, *35*, 1175−1179.

(4) Shah, R. R.; Merreceyes, D.; Husemann, M.; Rees, I.; Abbott, N. L.; Hawker, C. J.; Hedrick, J. L. *Macromolecules* **2000**, *33*, 597−605.

(5) Zhou, F.; Liu, W. M.; Hao, J. C.; Xu, T.; Chen, M.; Xue, Q. J. *Adv. Funct. Mater.* **2003**, *13*, 938−942.

(6) Balachandra, A. M.; Baker, G. L.; Bruening, M. L. *J. Membr. Sci.* **2003**, *227*, 1−14.

(7) Mayr, B.; Buchmeiser, M. R. *J. Chromatogr., A* **2001**, *907*, 73−80.

(8) Qin, S. H.; Qin, D. Q.; Ford, W. T.; Resasco, D. E.; Herrera, J. E. *Macromolecules* **2004**, *37*, 752−757.

(9) Guerrini, M. M.; Charleux, B.; Vairon, J. P. *Macromol. Rapid Commun.* **2000**, *21*, 669−674.

(10) Brantley, E. L.; Jennings, G. K. *Macromolecules* **2004**, *37*, 1476−1483.

(11) Dyer, D. J. *Adv. Funct. Mater.* **2003**, *13*, 667−670.

(12) Galli, P.; Vecellio, G. *J. Polym. Sci., Part A: Polym. Chem.* **2004**, *42*, 396−415.

(13) Benkoski, J. J.; Flores, P.; Kramer, E. J. *Macromolecules* **2003**, *36*, 3289−3302.

(14) Feldman, D. *J. Polym. Environ.* **2001**, *9*, 49−55.

(15) Cerofolini, G. F.; Galati, C.; Reina, S.; Renna, L. *Semicond. Sci. Technol.* **2003**, *18*, 423−429.

(16) Seshadri, K.; Atre, S. V.; Tao, Y. T.; Lee, M. T.; Allara, D. L. *J. Am. Chem. Soc.* **1997**, *119*, 4698−4711.

(17) Wang, X. S.; Lascelles, S. F.; Jackson, R. A.; Armes, S. P. *Chem. Commun.* **1999**, 1817−1818.

(18) Robinson, K. L.; Khan, M. A.; Banez, M. V. D.; Wang, X. S.; Armes, S. P. *Macromolecules* **2001**, *34*, 3155−3158.

(19) Jones, D. M.; Huck, W. T. S. *Adv. Mater.* **2001**, *13*, 1256−1259.

(20) Bontempo, D.; Tirelli, N.; Masci, G.; Crescenzi, V.; Hubbell, J. A. *Macromol. Rapid Commun.* **2002**, *23*, 418−422.

(21) Chen, X. Y.; Armes, S. P.; Greaves, S. J.; Watts, J. F. *Langmuir* **2004**, *20*, 587−595.

(22) Kim, J. B.; Huang, W. X.; Miller, M. D.; Baker, G. L.; Bruening, M. L. *J. Polym. Sci., Part A: Polym. Chem.* **2003**, *41*, 386−394.

(23) Gopireddy, D.; Husson, S. M. *Macromolecules* **2002**, *35*, 4218−4221.

(24) Qin, S. H.; Matyjaszewski, K.; Xu, H.; Sheiko, S. S. *Macromolecules* **2003**, *36*, 605−612.

(25) Khan, M.; Huck, W. T. S. *Macromolecules* **2003**, *36*, 5088−5093.

(26) Kraft, M. L.; Moore, J. S. *Langmuir* **2003**, *19*, 910−915.

(27) Rodriguezparada, J. M.; Kaku, M.; Sogah, D. Y. *Macromolecules* **1994**, *27*, 1571−1577.

(28) Riou, S. A.; Chien, B. T.; Hsu, S. L.; Stidham, H. D. *J. Polym. Sci. Part B: Polym. Phys.* **1997**, *35*, 2843−2855.

(29) Stöhr, T.; Rühe, J. *Macromolecules* **2000**, *33*, 4501−4511.

(30) Snyder, R. G.; Strauss, H. L.; Elliger, C. A. *J. Phys. Chem.* **1982**, *86*, 5145−5150.

(31) Zhang, D.; Shen, Y. R.; Somorjai, G. A. *Chem. Phys. Lett.* **1997**, *281*, 394−400.

(32) Fenter, P.; Eberhardt, A.; Liang, K. S.; Eisenberger, P. *J. Chem. Phys.* **1997**, *106*, 1600−1608.

(33) Neelakantan, A.; Stine, R.; Maranas, J. K. *Macromolecules* **2003**, *36*, 3721−3731.

(34) Laibinis, P. E.; Palmer, B. J.; Lee, S.-W.; Jennings, G. K. Self-Assembled Monolayers of Thiols. In *Thin Films*; Ulman, A.; Powell, R.; Francombe, M. H., Eds.; Academic Press: 1998; Vol. 24, pp 1−41 and references therein.

(35) Bain, C. D.; Troughton, E. B.; Tao, Y. T.; Evall, J.; Whitesides, G. M.; Nuzzo, R. G. *J. Am. Chem. Soc.* **1989**, *111*, 321−335.

(36) It has been shown that hexadecane may insert itself into a film that has defects at the surface, thus artificially raising the hexadecane contact angle and yielding a surface that appears to have densely packed methyl groups. Bicyclohexyl is often used to more clearly verify a methyl surface since it is unable to insert into a film due to its bulkiness but has only a slightly higher surface tension than hexadecane (32.8 vs 27.6). The advancing contact angle of bicyclohexyl on H15 and H17 was found to approach 53°, confirming the methyl functionality of these surfaces. See Bartell, L. S.; Ruch, R. J. *J. Phys. Chem.* **1959**, *63*, 1045−1049 or Bain et al.[35] for further information on this phenomenon.

(37) Fukushima, H.; Seki, S.; Nishikawa, T.; Takiguchi, H.; Tamada, K.; Abe, K.; Colorado, R.; Graupe, M.; Shmakova, O. E.; Lee, T. R. *J. Phys. Chem. B* **2000**, *104*, 7417−7423.

(38) This model also improves the fit for an unmodified PHEMA film, although the basic two-time-constant impedance model that we have used previously works very well. Resulting values for PHEMA film resistance and capacitance were not altered significantly, so the values from our previous work are reported herein for reference (Table 4).

(39) Bard, A. J.; Faulkner, L. R. *Electrochemical Methods: Fundamentals and Applications*, 2nd ed.; Wiley: New York, 2001.

(40) Park, S. M.; Yoo, J. S. *Anal. Chem.* **2003**, *75*, 455A−461A.

(41) Bantz, M. R.; Brantley, E. L.; Weinstein, R. D.; Moriarty, J.; Jennings, G. K. *J. Phys. Chem. B* **2004**, *108*, 9787−9794.